

荧光无机/有机杂化纳米分子口袋的构建

杨慧 刘礼兵 张洲 薛峥 李勇军 王树 刘辉彪*

(中国科学院化学研究所有机固体院重点实验室 北京分子科学国家实验室 北京 100190)

摘要 利用能量匹配原则将无机半导体 ZnO 纳米粒子与有机半导体四苯基卟啉四羧酸(TCPP)分子进行组装, 在无机-有机组分之间的界面构建了杂化纳米分子口袋 ZNPs-TCPP, 该纳米分子口袋对四苯基卟啉(TPP)分子具有高选择性识别功能, 同时其荧光增强了 5 倍以上, 并成功地将该杂化纳米分子口袋用于肺腺癌细胞(A549)的细胞成像。

关键词 纳米分子口袋; 卟啉; 无机/有机杂化; 细胞成像

Constructing High Luminescent Inorganic/Organic Hybrid Nanoscale Molecular Pockets

Yang, Hui Liu, Libing Zhang, Zhou Xue, Zheng
Li, Yongjun Wang, Shu Liu, Huibiao*(CAS Key Laboratory of Organic Solids, Beijing National Laboratory for Molecular Sciences (BNLMS),
Institute of Chemistry, Chinese Academy of Sciences, Beijing 100190, China)

Abstract An inorganic/organic hybrid nanoscale molecular pocket ZNPs-TCPP was constructed through the assembly of 5,10,15,20-tetra(3-carboxyphenyl) porphyrin (TCPP) on the surface of ZnO nanoparticles (NPs), which highly selectively recognized 5,10,15,20-tetraphenylporphyrin (TPP) molecule. The resulting hybrid nanoscale molecular pockets ZNPs-TCPP captured TPP demonstrated high emission efficiency and the intensity of its emission was five times greater than that of ZnONPs-TCPP. Significantly, the molecular pocket ZNPs-TCPP-TPP with high luminescence can be dispersed in water and is successfully applied for the cell imaging of A549.

Keywords nanoscale molecular pockets; porphyrin; inorganic/organic hybrid; cell imaging

1 Introduction

Inorganic/organic hybrid nanomaterials (IOHN) consisting of organic and inorganic nanomaterials can be chemically or biologically active species, providing favourable applied perspectives through tuneable optics, electronics, electrics and photo-electrics, which may exhibit properties and functions unattainable in the individual components^[1]. In the case, the IOHN requires fine-tuning of the sizes, morphologies, and spatial assembly of individual domains and their interfaces. These factors will impact the chemical properties required for functionality^[2]. In other cases the materials are linked through molecular interactions which influence the electronic and physical properties of the materials used to prepare the IOHN^[2]. Specifically, tuning the structure and interface interactions within the IOHN has resulted in producing a novel properties or improving the optical and electrical properties. The major advantage of ION over the alone organic or inorganic component is the increase of active surface area and ability to form good electronic contact between the organic and inorganic components. Although considerable research efforts have been put into the design of suitable organic

molecules, which respect to the “how” the secondary component (inorganic products) is incorporated in the organic units and “how” controlled the matching of the structures and the energy between inorganic and organic molecules is difficultly reached. Generally, a particularly attractive issue with IOHN is the modulation of the fluorescence. However, the fluorescence of many IOHN can be quenched due to adsorption of organic ligands on the surface of inorganic nanoparticles, which leads to hindering their application, especially for biological imaging and labelling.

Although Cd-based quantum dots such as CdSe and CdSe/ZnS nanoparticle are of intense interest in their potential applications as probes for biological imaging and labeling^[3], the Cd-based nanoparticles are toxic to cells even at very low concentrations, due to the release of Cd²⁺ ions into the cellular environment^[4]. As probes for biological imaging and labeling, ZnO nanoparticles (NPs) have been considered as one of the good candidates for the alternatives to Cd-based NPs, because ZnO NPs are nontoxic, biocompatible and environmentally-benign fluorophores^[5]. Importantly, the optical properties of ZnO NPs can be controlled through introducing organic molecules

* E-mail: liuhb@iccas.ac.cn

Received August 25, 2014; published December 9, 2014.

Supporting information for this article is available free of charge via the Internet at <http://sioc-journal.cn>

Project supported by the National Natural Science Foundation of China (Nos. 21373235, 21031006) and the National Basic Research Program of China (Nos. 2011CB932302, 2011CB932303).

项目受国家自然科学基金(Nos. 21373235, 21031006)和国家重点基础研究计划(Nos. 2011CB932302, 2011CB932303)资助。

on the surface of ZnO NPs by covalently linking^[6]. As a matter of fact, the emission efficiency of ZnO NPs is low, which blocks their extensive application in biological imaging. During the past decade, scientists have tried to develop techniques to introduce organic fluorophores to modify ZnO NPs for improving the emission efficiency^[7,8]. Unfortunately, the successes of case are a few, due to the electronics and energy transfer between ZnO NPs and organic fluorophores results in quenching the fluorescence. Still, the design and synthesis of nanoscale IOHN with high luminescence is a significant and ongoing challenge.

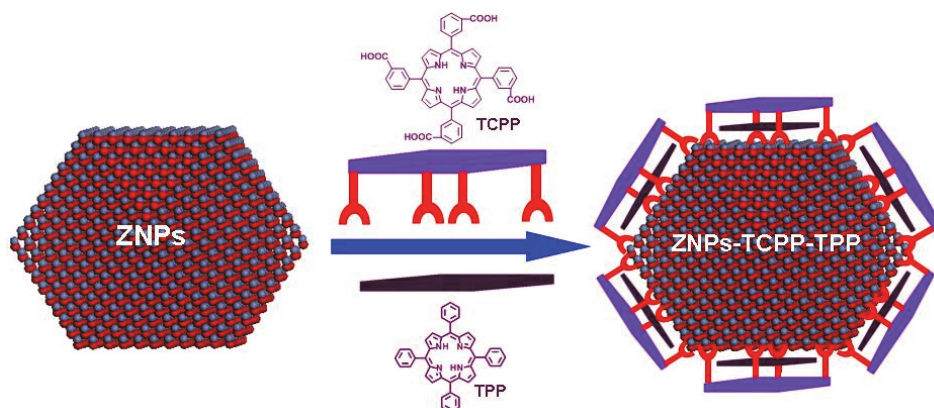
Here, we develop a novel strategy for synthesizing nanoscale molecular pocket, based on inorganic/organic hybrid nanostructures, through interfacial attraction between organic functional molecules and inorganic semiconductor nanoparticles. In this approach, organic guest molecules are first physically adsorbed onto the surfaces of ZNPs; next, the 5,10,15,20-tetra(3-carboxyphenyl) porphyrin (TCPP) captures the adsorbed guest molecules by self-assembly, fixing them to the surface of ZnO NPs. The assembled TCPP units on the surfaces of ZnO NPs possess pocket-like interfacial cavities (named “molecular pockets”), in which the carboxylate groups of TCPP can strongly coordinate with the zinc ions on the surfaces of the ZnO NPs, and this cavity was readily loaded with the planar organic molecules. The hybrid nanoscale molecular pocket exhibits highly selective recognition of TPP, with the resulting ZNPs-TCPP-TPP system displaying high emission efficiency—the intensity of its emission signal was five times greater than that of ZNPs-TCPP. Because of its high dispersibility in water, we applied the molecular pocket ZNPs-TCPP-TPP to the imaging of A549 cells.

2 Results and discussion

ZnO NPs with an average diameter *ca.* 4 nm were prepared by a sol-gel technique^[9]. TCPP were synthesized as reported^[10]. The molecular pocket ZNPs-TCPP was constructed by mixed the TCPP ethanol solution of 1×10^{-6} mol/L and ZnO NPs colloids of 0.2 g/mL. The molecular pocket (ZNPs-TCPP-TPP) for selectively captured TPP molecule was produced as follows (Scheme 1). TEM and HRTEM images (Figure S1 in Supporting Information) display that ZNPs-TCPP with diameter of about 4 nm possess a good dispersity in ethanol. The ethanol solution of

TPP (1×10^{-5} mol/L) firstly mixed with ZnO NPs colloids of 0.2 g/mL. Then, the ethanol solution of TCPP was added into the colloids of TPP and ZnO NPs. After the resulted mixture was treated with ultrasonic for 20 min, the mixture was centrifuged and washed with ethanol for three times to achieve the molecular pocket ZNPs-TCPP-TPP. The molecular pocket of ZNPs-TCPP-TPP was able to be dispersed into ethanol. The absorption spectrum (Figure 1a) shows that the band of ZNPs-TCPP at 327 nm lightly shifts to 331 nm comparing to ZnO NPs and the features typical of TCPP ring at 426 nm (the Soret band) and at 516 nm, 558 nm [Q(1,0) bands] and 589 nm [Q(0,0) band] were observed. The addition of TPP results in an obvious blue shift of Soret band to 414 nm and the intensity of absorption increasing over four times. The shoulder at 396 nm on the high energy side of the Soret band indicated the face-to-face aggregation between TCPP and TPP^[11]. The absorption intensities of Q bands also enhanced distinctly. The Q(1,0) bands at 516 nm and 558 nm shift to 510 nm and 550 nm and the Q(0,0) band at 589 nm shifts to 595 nm. A band at 646 nm on the low energy side of Q(0,0) band was observed. This phenomenon is due to exciton coupling between adjacent TPP and TCPP at the surface of ZNPs. When perylene, pyrene, and anthracene were added into ZNPs-TCPP, respectively, the intensity of absorption slightly increased. The results indicated that ZNPs-TCPP exhibited a selective recognition to TPP molecule in solution.

Figure 1b shows the emission spectra of TCPP, ZNPs-TCPP and ZNPs-TCPP-TPP ($\lambda_{\text{ex}} = 415$ nm) in ethanol, respectively. TCPP exhibits typical emission at 652 nm and 713 nm. On the fluorescence spectra of ZNPs-TCPP, the emission at 652 nm obviously decreases due to electron injection into the conduction band of ZnO. When TPP was added, the emissions of ZNPs-TCPP-TPP at 652 nm and 713 nm increased about 6.5 and 5.4 times of ZNPs-TCPP, respectively. The results indicated that ZNPs-TCPP displayed a selective turn-on fluorescence response to TPP molecule in solution. For determining the selectivity of ZNPs-TCPP to TPP, the competition experiments of ZNPs-TCPP with TPP and polycyclic aromatic hydrocarbons (PAHs), such as perylene, pyrene, anthracene *etc.*, respectively, shows that the emissions of ZNPs-TCPP at 652 nm slightly enhanced (Figure 1b). However, when the mixture of TPP and PAHs was added,



Scheme 1 Construction of the molecular pocket ZNPs-TCPP-TPP

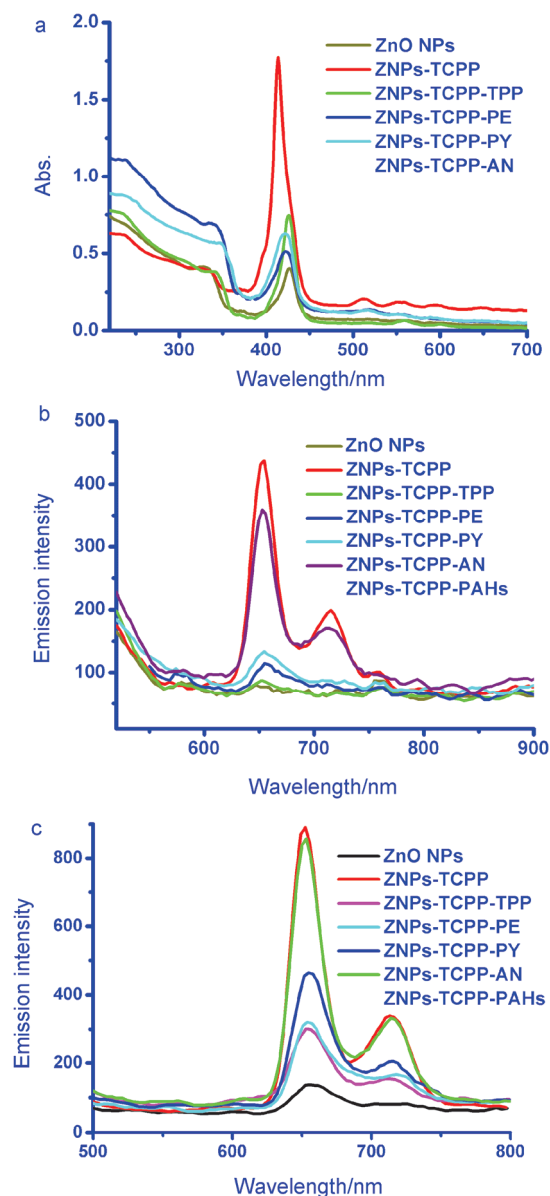
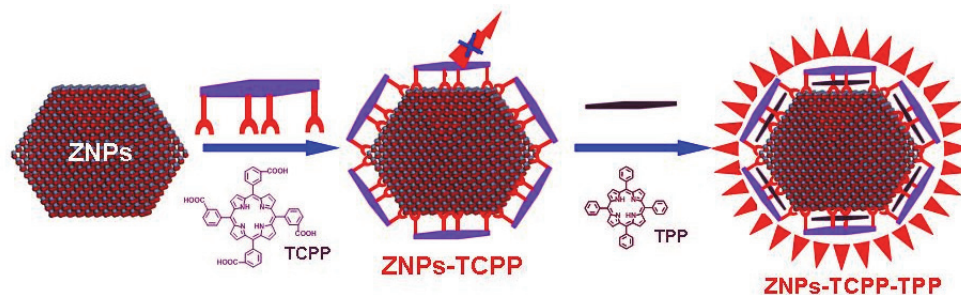


Figure 1 (a) The absorption spectra of ZnO NPs, ZNPs-TCPP, ZNPs-TCPP, ZNPs-TCPP-TPP and ZNPs-TCPP added perylene (PE), pyrene (PY) and anthracene (AN) in ethanol solution, respectively. (b, c) The fluorescence spectra of ZnO NPs, ZNPs-TCPP, ZNPs-TCPP, ZNPs-TCPP-TPP and ZNPs-TCPP added perylene (PE), pyrene (PY), anthracene (AN) and PAHs (mixture of TPP, PE, PY and AN) in ethanol solution, respectively. (b) $\lambda_{\text{ex}}=415$ nm. (c) $\lambda_{\text{ex}}=505$ nm

the emissions at 652 nm and 713 nm strongly increased, which indicated the excellent selectivity for TPP over these PAHs (Figure 1b). When $\lambda_{\text{ex}}=505$ nm, the emissions of ZNPs-TCPP-TPP at 652 nm and 713 nm also strongly increased (Figure 1c).

As shown in Scheme 2, the molecular pocket of ZNPs-TCPP on the interface of inorganic (ZnO NPs)/organic (TCPP molecule) hybrid nanomaterials is formed via the interactions between the Zn^{2+} cations on the surface of the inorganic ZnO NPs and the carboxylate anions of TCPP unit. There are hardly interactions between porphyrin ring of TCPP and Zn^{2+} of ZnO NPs because the four meta-substituted benzoic acid groups of TCPP are not coplanar with the porphyrin ring and the latter was positioned relatively distant from the Zn^{2+} ions on the surface of the ZnO. The size of molecular pocket is suitable for loading TPP molecule through π - π interactions between porphyrin framework of TPP and TCPP, which is stronger than that of PE, PY and AN. In addition, the interaction of TPP and Zn^{2+} in ZnO NPs leads to greatly increasing the recognition ability for TPP molecule in molecular pocket. A possible process for the high emission of ZNPs-TCPP-TPP is as follows. When the TCPP is bound to ZnO NPs, the fluorescence of ZnO NPs and TCPP are quenched owing to the electron of TCPP injection into the conduction band of ZnO under photo-excitation^[12,11c]. After molecular pocket ZNPs-TCPP captured PAHs, electron transfer directly from PE, PY, and AN to TCPP due to among of their strong π -stacking interactions. The accumulation of electrons on the TCPP unit resulted in more electrons transferring to the ZnO NPs, which leads to the complete quenching of the emissions of the ZnO. For TPP, the guest molecule is positioned relatively close to the surface of the ZnO NPs after loading into the molecular pocket ZNPs-TCPP, favoring coordination interactions between TPP and Zn^{2+} ions of ZnO NP, which results in restoring the emission of the TCPP unit. Simultaneously, in the molecular pocket, the overlapping of the UV-Vis absorption bands of TCPP and TPP also greatly enhanced the emission of ZNPs-TCPP-TPP.

Time-resolved fluorescence measurements monitored at the wavelength above 500 nm, were performed for the fluorescence lifetimes information on the charge-transfer dynamics in the ZNPs-TCPP-TPP (Figure 2). The measurements revealed that the fluorescence of TCPP and TPP showed lifetime of 9.87 ns and 10.97 ns, respectively. The fluorescence lifetime of ZNPs-TCPP decreased to 8.61 ns



Scheme 2 Schematic illustration of molecule pocket for selectively sensing TPP

(Figure 2). After captured TPP to form ZNPs-TCPP-TPP, the fluorescence lifetime increased to 9.63 ns. The faster fluorescence decay of ZNPs-TCPP can be attributed to the strong interactions between TCPP and ZnO in ZNPs-TCPP, where it is easy for the exciton to find the interface and dissociate, representing as a rapid electron injection from TCPP to the conduction band of ZnO^[13]. The result is consistent with the static fluorescence measurement. The lifetime of ZNPs-TCPP-TPP was 9.63 ns, which is longer than that of ZNPs-TCPP and shorter than that of TPP. The result showed the electron injection is from TPP to the conduction band of ZnO due to the improved interfacial contact between TPP and the surface of ZnO in ZNPs-TCPP-TPP. TPP hindered the electron injection from TCPP to ZnO, which lead to the restoration of fluorescence of TCPP.

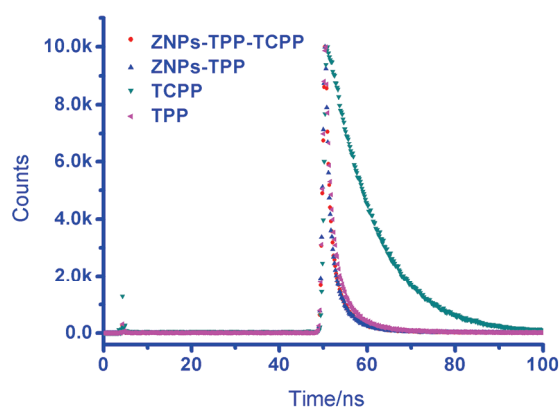


Figure 2 Time resolved nanosecond fluorescence spectroscopy of ZNPs-TCPP-TPP, ZNPs-TCPP, TCPP and TPP, $\lambda_{\text{ex}}=375$ nm and $\lambda_{\text{em}}=650$ nm

The ZNPs-TCPP-TPP is successfully applied in cell imaging due to its dispersion in water and strong fluorescence. Figure 3a-b show that the ZNPs-TCPP-TPP can image human pulmonary adenocarcinoma cell (A549) including nuclear. Furthermore, the cellular multilabeling

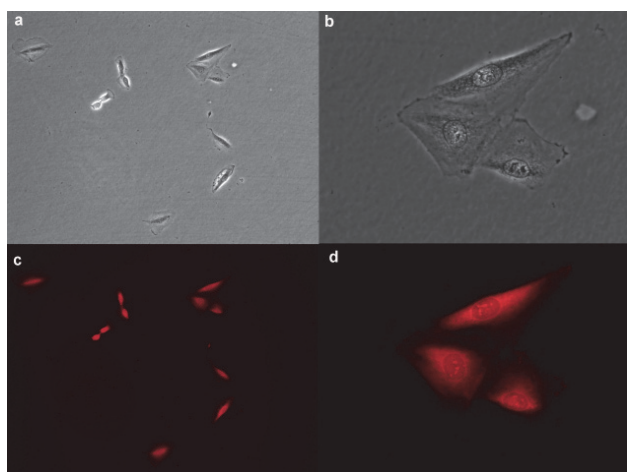


Figure 3 Phase contrast (a), (b) and fluorescence microscopy (c), (d) images of ZNPs-TCPP-TPP for cell image. Fluorescence images of ZNPs-TCPP-TPP were recorded on fluorescence microscopy (Olympus IX71) using a D455/70 nm excitation filter and D600/50 nm emission filter with 100 ms exposure time

and multianalysis can be realized by the multicolor characteristic of stable supramolecular system of ZNPs-TCPP-TPP under the irradiation of visible light. As shown in Figure 3c-d, the ZNPs-TCPP-TPP-stained A549 cells exhibit bright and clearly resolved fluorescence.

3 Conclusion

In summary, we have developed a novel strategy to construct the inorganic/organic hybrid nanoscale molecular pocket ZNPs-TCPP formed through the assembly of TCPP and ZnO NPs. The nanoscale molecular pocket ZNPs-TCPP exhibited high selectivity in the recognition of TPP and displayed high emission efficiency, the emission intensity of which increased over five times relative to that of ZNPs-TCPP. The hybrid nanoscale molecular pocket ZNPs-TCPP-TPP showed high dispersion ability in water and strong luminescence, we applied this species successfully to cell imaging of A549. This strategy opens a door for the construction of novel solid state supramolecular systems with high luminescence based on inorganic/organic hybrid nanostructures, which will be expected potential application for various bio-applications, such as fluorescent biological probes *etc.*

4 Experimental section

4.1 Materials and instruments

All of reagents and solvents were purchased from Beijing Chemical reagent Corporation, China, Acros or Aldrich Corp. and were utilized as received unless indicated otherwise. UV-vis spectra were taken on a Hitachi U-3010 spectrometer, and fluorescence spectra were measured on a Hitachi F-4500 spectro-fluorometer. Time-resolved fluorescence spectra were measured using a photo-counting streak camera (C2909, a mamatstu). This machine uses a femto-second laser source running at 1 kHz. The laser's output wavelength can be set to the desired excitation with OPA-800CF, Spectra Physics). The fluorescence lifetimes were measured on an Edinburgh Instruments Ltd FLS920. Transmission electron microscopy (TEM) measurements were conducted with JEOL 2010 transmission electron microscopes using an accelerating rate voltage of 200 keV.

4.2 Synthesis of molecular pocket ZNPs-TCPP

ZnO NPs with an average diameter *ca.* 4 nm were prepared by a sol-gel technique^[9]. 5,10,15,20-tetra(3-carboxyphenyl) porphyrin (TCPP) were synthesized as reported^[10]. Under ultrasonic bath for 20 min, 0.2 mg dry ZnO NPs was dispersed into 1 mL ethanol to form colloid. The molecular pocket ZNPs-TCPP was synthesized by mixed 1 mL TCPP ethanol solution of 1×10^{-5} mol/L and ZnO NPs colloids of 0.2 g/mL for 10 min under ultrasonic bath. The mixture was centrifugated and washed by ethanol for three times. The colloid of ZNPs-TCPP was prepared by re-dispersing the remains into 2 mL ethanol.

4.3 Synthesis of molecular pocket ZNPs-TCPP-TPP

The molecular pocket ZNPs-TCPP-TPP was synthesized by mixed 1 mL TPP ethanol solution of 1×10^{-5} mol/L and ZNPs colloids of 0.2 g/mL for 20 min under ultrasonic bath. And then, TCPP 1 mL ethanol solution of 1×10^{-5}

mol/L was added for 20 min under ultrasonic bath. The mixture was centrifugated and washed by ethanol for three times. The colloid of ZNPs-TCPP-TPP was prepared by re-dispersing the remains into 2 mL ethanol for measurements of UV absorption spectra, fluorescent spectra, time resolved nanosecond fluorescence spectroscopy and TEM. For sensing TPP, PAHs (1 mL) (included 10^{-5} mol/L perylene, anthracene, pyrene and TPP) were added to 1 mL ZnO NPs colloids (0.2 g/mL) in ultrasonic bath for 30 min. And then, TCPP 1 mL ethanol solution of 1×10^{-5} mol/L was added for 20 min under ultrasonic bath. The mixtures were centrifugated and washed by ethanol three times. The colloid of ZNPs-TCPP-TPP was obtained by re-dispersing the remains into 2 mL ethanol for measurements of UV absorption spectra and fluorescent spectra.

4.4 Cell imaging

Human pulmonary adenocarcinoma cell (A549) was purchased from cell culture center of Institute of Basic Medical Sciences, CAMS and cultured in Dulbecco's Modified Eagle's Medium, High Glucose (DMEM) supplemented with 10% neonatal bovine serum (NBS). Neonatal bovine serum was purchased from Sijiqing Biological Engineering Materials (Hangzhou, China). Liquid cell culture medium was purchased from HyClone/Thermo-fisher (Beijing, China). Cell cultural consumables were purchased from Nunc (HuameiBio, Beijing). A549 cells were routinely cultured in DMEM (high glucose) medium containing 10% NBS and harvested for subculture using trypsin (0.05%, Gibco/Invitrogen) and grown in a humidified atmosphere containing 5% CO₂ and 95% air at 37 °C. Before experiment, the cells were pre-cultured until confluence was reached. The cells were seeded in 35 mm culture plates (Nunc) at a density of approximately 1×10^5 cells per plate. After 24 h, the medium was removed and the adherent cells were washed once with $1 \times$ PBS and fixed by 75% ethanol with 2 μmol/L ZNPs-TCPP-TPP colloid of water for 20 min at room temperatures. The cell monolayer was washed twice with $1 \times$ PBS buffer and imaged by fluorescence microscopy (Olympus IX71) and 100 ms exposure time. The type of light filter is D455/70 nm exciter, 570 nm beam splitter, and D600/50 nm emitter.

References

- [1] (a) Sanchez, C.; Shea, K. J.; Kitagawa, S. *Chem. Soc. Rev.* **2011**, *40*, 471; (b) Zheng, H. Y.; Li, Y. J.; Liu, H. B.; Yin, X. D.; Li, Y. L. *Chem. Soc. Rev.* **2011**, *40*, 4506; (c) Guo, Y. B.; Liu, H. B.; Li, J. L.; Li, G. X.; Zhao, Y. J.; Song, Y. L.; Li, Y. L. *J. Phys. Chem. C* **2009**, *113*, 12669; (d) Guo, Y. B.; Tang, Q. X.; Liu, H. B.; Zhang, Y. J.; Li, Y. L.; Hu, W. P.; Wang, S.; Zhu, D. B. *J. Am. Chem. Soc.* **2008**, *130*, 9298; (e) Liu, H. B.; Cui, S.; Guo, Y. B.; Li, Y. L.; Huang, C. S.; Zuo, Z. C.; Yin, X. D.; Song, Y. L.; Zhu, D. B. *J. Mater. Chem.* **2009**, *19*, 1031; (f) Law, M.; Greene, L. E.; Johnson, J. C.; Saykally, R.; Yang, P. *Nat. Mater.* **2005**, *4*, 1; (g) Park, S.; Chung, S.-W.; Mirkin, C. A. *J. Am. Chem. Soc.* **2004**, *126*, 11772; (h) Xu, X.; Goponenko, A. V.; Asher, S. A. *J. Am. Chem. Soc.* **2008**, *130*, 3113; (i) Huang, X.; Li, J. *J. Am. Chem. Soc.* **2007**, *129*, 3157; (j) Climent, E.; Marcos, M. D.; Martínez-Máñez, R.; Sancenón, F.; Soto, J.; Rurack, K.; Amorós, P. *Angew. Chem. Int. Ed.* **2009**, *48*, 8519; (k) Liu, H. B.; Xu, J. L.; Li, Y. J.; Li, Y. L. *Acc. Chem. Res.* **2010**, *43*, 1469; (l) Chen, N.; Chen, S. H.; Ouyang, C. B.; Yu, Y. W.; Liu, T. F.; Li, Y. J.; Liu, H. B.; Li, Y. L. *NPG Asia Mater.* **2013**, *5*, e59; (m) Lin, H. W.; Liu, H. B.; Qian, X. M.; Chen, S. H.; Li, Y. J.; Li, Y. L. *Inorg. Chem.* **2013**, *52*, 6969; (n) Liu, H. B.; Wang, K.; Zhang, L.; Qian, X. M.; Li, Y. J.; Li, Y. L. *Dalton Trans.* **2014**, *43*, 432; (o) Li, Y. J.; Liu, T. F.; Liu, H. B.; Tian, M.-Z.; Li, Y. L. *Acc. Chem. Res.* **2014**, *47*, 1186; (p) Zhu, W. G.; Zhang, D. Z.; Fu, H. B. *Acta Chim. Sinica* **2012**, *70*, 2337. (朱伟钢, 张德忠, 付红兵, 化学学报, **2012**, *70*, 2337.)
- [2] (a) Huynh, W. U.; Dittmer, J. J.; Alivisatos, A. P. *Science* **2002**, *295*, 2425; (b) Dahan, M.; Levi, S.; Luccardini, C.; Rostaing, P.; Riveau, B.; Triller, A. *Science* **2003**, *302*, 442; (c) Snee, P. T.; Somers, R. C.; Nair, G.; Zimmer, J. P.; Bawendi, M. G.; Nocera, D. G. *J. Am. Chem. Soc.* **2006**, *128*, 13320; (d) Polleux, J.; Pinna, N.; Antonietti, M.; Niederberger, M. *J. Am. Chem. Soc.* **2005**, *127*, 15595; (e) Shavel, A.; Arbiol, J.; Cabot, A. *J. Am. Chem. Soc.* **2010**, *132*, 4514; (f) Xu, Y.; Yuan, J.; Fang, B.; Drechsler, M.; Müllner, M.; Bolisetty, S.; Ballauff, M.; Müller, A. H. E. *Adv. Funct. Mater.* **2010**, *20*, 4182; (g) He, X. R.; Liu, H. B.; Li, Y. L.; Wang, S.; Li, Y. J.; Wang, N.; Xiao, J. C.; Xu, X. H.; Zhu, D. B. *Adv. Mater.* **2005**, *17*, 2811; (h) Descalzo, A. B.; Martínez-Máñez, R.; Sancenón, F.; Hoffmann, K.; Rurack, K. *Angew. Chem. Int. Ed.* **2006**, *45*, 5924; (i) Han, W. S.; Lee, H. Y.; Jung, S. H.; Lee, S. J.; Jung, J. H. *Chem. Soc. Rev.* **2009**, *38*, 1904.
- [3] (a) Medintz, L. L.; Uyeda, H. T.; Goldman, E. R.; Mattoussi, H. *Nat. Mater.* **2004**, *4*, 435; (b) De, M.; Ghosh, P. S.; Rotello, V. M. *Adv. Mater.* **2008**, *20*, 1; (c) Rogach, A. L.; Kornowski, A.; Karshaw, S. V.; Brot, M.; Harrison, M.; Eychmüller, A. *Adv. Mater.* **1999**, *11*, 552; (d) Peng, Z.; Peng, X. *J. Am. Chem. Soc.* **2001**, *123*, 183.
- [4] (a) Kirchner, C.; Liedl, T.; Kudara, S.; Pellegrino, T.; Muñoz Javier, A.; Gaub, H. E.; Stölzle, S.; Fertig, N.; Parak, W. J. *Nano Lett.* **2005**, *5*, 331; (b) Song, Y. C.; Liu, J. X.; Zhang, Y. Y.; Shi, W.; Ma, H. M. *Acta Chim. Sinica* **2013**, *71*, 1607. (宋延超, 刘俊秀, 张阳阳, 史文, 马会民, 化学学报, **2013**, *71*, 1607); (c) Qian, X. M.; Liu, H. B.; Li, Y. L. *Chin. Sci. Bull.* **2013**, *58*, 2686.
- [5] (a) Mattoussi, H.; Mauro, J. M.; Goldman, E. R.; Anderson, G. P.; Sunder, V. C.; Mikulec, F.; Bawendi, M. G. *J. Am. Chem. Soc.* **2000**, *122*, 12142; (b) Hong, R.; Fischer, N. O.; Verma, A.; Goldman, C. M.; Emrich, T.; Rotello, V. M. *J. Am. Chem. Soc.* **2004**, *126*, 739.
- [6] (a) Chan, W. C. W.; Nie, S. *Science* **1998**, *281*, 2016; (b) Bruchez Jr., M.; Moronne, M.; Gin, P.; Weiss, S.; Alivisatos, A. P. *Science* **1998**, *281*, 2013.
- [7] (a) Marczak, R.; Werner, F.; Gnichwitz, J. F.; Hirsch, A.; Guldi, D. M.; Peukert, W. *J. Phys. Chem. C* **2009**, *113*, 4669; (b) Derfus, A. M.; Chan, W. C. W.; Bhatia, S. N. *Nano Lett.* **2004**, *4*, 11; (c) Oosterhout, S. D.; Wienk, M. M.; van Bavel, S. S.; Thiedmann, R.; Koster, L. J. A.; Gilot, J.; Loos, J.; Schmidt, V. J.; Janssen, R. A. *Nat. Mater.* **2009**, *8*, 818; (d) Beek, W. J. E.; Wienk, M. M.; Janssen, R. A. *J. Adv. Funct. Mater.* **2006**, *16*, 1112.
- [8] Liu, H. B.; Zuo, Z. C.; Guo, Y. B.; Li, Y. J.; Li, Y. L. *Angew. Chem. Int. Ed.* **2010**, *49*, 2705.
- [9] Pacholski, C.; Kornowski, A.; Weller, H. *Angew. Chem. Int. Ed.* **2002**, *41*, 1188.
- [10] Bonar-Law, R. P.; Sanders, J. J. *Chem. Soc. Chem. Commun.* **1991**, 575.
- [11] (a) Rochford, J.; Chu, D.; Hagfeldt, A.; Galoppini, E. *J. Am. Chem. Soc.* **2007**, *129*, 4655; (b) Rochford, J.; Galoppini, E. *Langmuir* **2008**, *24*, 5366.
- [12] (a) Kalyanasundaram, K.; Gratzel, M. *Coord. Chem. Rev.* **1998**, *177*, 347; (b) Stromberg, J. R.; Marton, A.; Kee, H. L.; Kirmaier, C.; Diers, J. R.; Muthiah, C.; Taniguchi, M.; Lindsey, J. S.; Bocian, D. F.; Meyer, G. J.; Holten, D. *J. Phys. Chem. C* **2007**, *111*, 15464.
- [13] (a) Sun, B.; Snaith, H. J.; Dhoot, A. S.; Westenhoff, S.; Greenham, N. C. *J. Appl. Phys.* **2005**, *97*, 014914; (b) Kang, Y. M.; Park, N. G.; Kimm, D. W. *Appl. Phys. Lett.* **2005**, *86*, 113101.

(Cheng, B.)